Correspondence

Adaptive Subband Transforms in Time-Frequency Excisers for DSSS Communications Systems

Mehmet V. Tazebay and Ali N. Akansu

Abstract—**A smart time-frequency exciser for DSSS communications is proposed in this correspondence. This technique utilizes the concept of uncertainty in time-frequency analysis of signals. It brings the novel concept of domain switchable signal processing. Hence, the adaptive time-frequency (ATF) exciser has the capability of deciding the domain of the interference cancellation. Additionally, adaptive subband transforms are utilized for frequency domain excision. For time-domain excision, the ATF excision algorithm utilizes a sliding time window to reject the nonstationary, pulsed (time-localized) interference. It is shown that the proposed adaptive time-frequency exciser-based DSSS communications receiver drastically outperforms the existing systems. Its performance is nearly optimal and very robust to the inter and intradomain variations of the undesired signal.**

I. Introduction

Spread spectrum modulation techniques produce a transmitted frequency spectrum that is much wider than the information bandwidth. This increase in bandwidth yields a processing gain that provides desired features such as interference suppression, code-division multiple access, energy density reduction, and good time resolution in digital communications systems [1]. However, the interference rejection capability of spread spectrum systems is limited. Both deliberate and unintentional interference (jamming) can be rejected up to a certain jamming margin. Among different spreading techniques, the direct sequence spread spectrum (DSSS) or pseudo-noise (PN) modulation system is considered in this study.

The DSSS transmitter, which is shown in Fig. 1, spreads the incoming data bit stream d_l ($d_l \in \{-1, 1\}$, $\forall l$) and, therefore, its spectrum by multiplying it with the spreading sequence $\underline{c}$ ($c_i \in \{-1, 1\}$ for $i = 1, \ldots K$). During the transmission, the channel adds a noise term $\underline{n}_l$ and other interferences $\underline{j}_l$. Therefore, the received signal $\underline{r}_l$ can be written as

$$\underline{r}_l = d_l \underline{c} + \underline{j}_l + \underline{n}_l. \tag{1}$$

The data bit stream d_l has a bit-to-bit duration of T_d s. The PN spreading code has a chipping rate of T_c s, where $T_d \gg T_c$. Hence, the length of the PN code is obtained as $K = \frac{T_d}{T_c}$. Without any interfering signal $\underline{j}_l$, the transmitted DSSS signal has a flat spectrum. The receiver correlates the signal with a properly synchronized version of the spreading sequence $\underline{c}$. The length-K PN spreading code has the energy $\underline{c}\,\underline{c}' = \sum_{i=1}^{K} c^2(i) = K$. The decision variable is therefore obtained as

$$\begin{aligned} U_l &= \underline{r}_l\,\underline{c}' = d_l \underline{c}\,\underline{c}' + \underline{j}_l\,\underline{c}' + \underline{n}_l\,\underline{c}' \\ &= K d_l + \underline{j}_l\,\underline{c}' + \underline{n}_l\,\underline{c}'. \end{aligned} \tag{2}$$

Manuscript received August 4, 1994; revised March 28, 1995. This work was supported by GEC-Marconi. The associate editor coordinating the review of this paper and approving it for publication was Dr. Truong Q. Nguyen.

The authors are with the Department of Electrical and Computer Engineering, Center for Communications and Signal Processing Research, New Jersey Institute of Technology, Newark, NJ 07102 USA.

IEEE Log Number 9415089.

Equation (2) indicates that the despreading operation recovers the desired signal while spreading the interference. In fact, if the interference power is greater than the system's jamming margin, the DSSS receiver fails to operate. The interference immunity of a DSSS receiver can be further improved by suppressing or excising $\underline{j}_l$ in (1) before despreading. Two classes of narrowband interference rejection schemes for DSSS communications have been extensively studied in the literature: least mean square estimation techniques, and transform domain processing structures [2], [3].

In the first approach, the coefficients of the excision filter can be obtained optimally (in the minimum mean square sense) from Wiener–Hopf equations if the statistics of the desired signal, interference, and noise are known. However, in practice, it is only possible to estimate these statistics. This leads to adaptive forms of these equations, which are not necessarily optimal.

Transform domain excision techniques often utilize a fixed transform, such as a discrete Fourier transform (DFT), to map the signal into the frequency domain. Independently, the eigenanalysis-based excision technique has also been proposed for narrowband interference excision in DSSS communications. This indeed is the optimal block transform, Karhunen-Loeve transform (KLT)-based excision technique. However, its performance is limited by the transform size or resolution. More recently, better frequency localized subband transforms over the conventional block transforms have been employed for interference excision in DSSS communications [4], [9]. It is naturally observed that fixed subband transforms have similar limitations as block transforms, such as interband spectral leakage and fixed time-frequency resolution. Particularly, for nonstationary interferers such as spikes, transform domain-based techniques fail [7].

The proposed smart ATF exciser carries out an efficient examination of time and frequency domain properties of the received signal. It first identifies the localization of interference and suppresses it in the proper domain. Additionally, it overcomes the fixed spectral resolution problem of existing transform domain-based excision techniques by employing the adaptive subband tree structuring concept.

In Section II, the adaptive subband transforms is discussed. In Section III, the proposed ATF exciser is explained in detail. Finally, in Section IV, performance results are given. The issue of robust performance is discussed, and conclusions are made.

II. Adaptive Subband Transforms

By their nature, subband transforms emphasize multirate signal processing. Flexibilities like multiresolution, unequal bandwidth, and different time durations are possible. The conventional subband transforms do not have any flexibility to adapt their time-frequency properties to the time-varying input signal. Therefore, their decomposition or compaction performance depends on the input spectrum. Their energy compaction degrades significantly if the input spectrum mismatches the spectral properties of the basis functions. This brings us to the robustness issue, which is critical in applications. On the other hand, it was well recognized that a blind M-band decomposition of an input spectrum does not always yield performance improvement. The magnitude responses of progressively optimized 64-band PR-QMF's are shown in Fig. 2 [5]. Although paraunitary conditions or completeness properties are satisfied, the interband spectral leakage

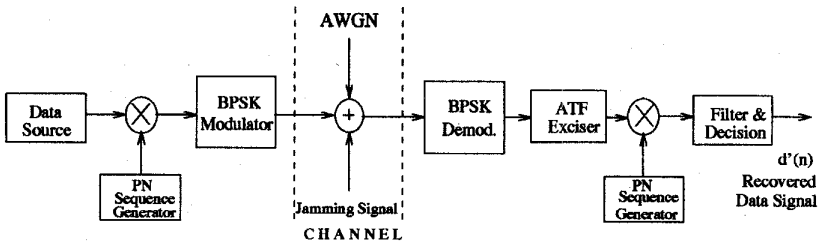

Fig. 1. Block diagram of a direct sequence spread spectrum system.

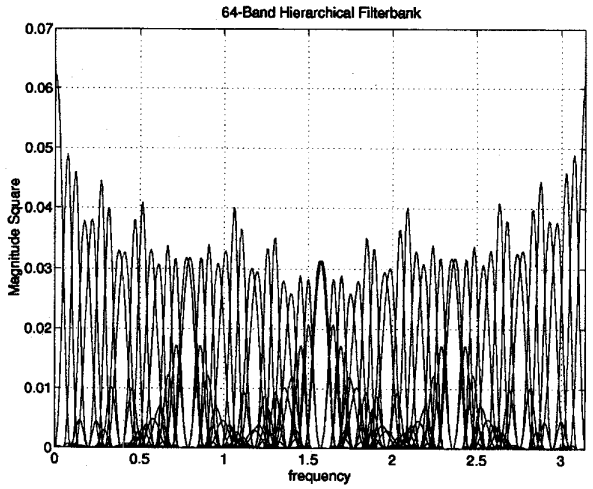

Fig. 2. Frequency responses of progressively optimized hierarchical 64-band product filters $[0, \pi]$ [5].

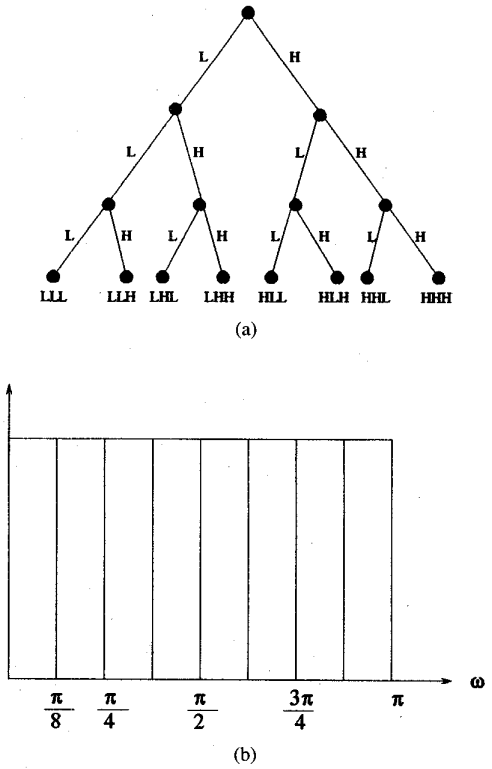

Fig. 3. (a) Regular subband tree structure; (b) equal bandwidth eight-band spectra.

occurs, and it can be minimized down to a certain limit. Therefore, the basis selection for the decomposition is very critical.

As an alternative to the M-band direct filter bank structure, the conventional hierarchical M-band subband trees achieve the spectral split by using the same prototype 2-band PR-QMF in multiple stages. Fig. 3 displays a regular hierarchical subband tree and corresponding ideal spectral split. A dyadic tree structure and its subbands are given in Fig. 4. The irregular subband tree is given in Fig. 5, along with its subspectra. The irregular tree is the most flexible one, and it implies a better tuning of the linear transform basis to the signal spectrum under consideration. Additionally, it suggests computational reductions since unnecessary decomposition steps are not performed.

By utilizing a tree structuring algorithm, an adaptive subband transform can effectively track the spectral variations of the input signal. The concept of tree structuring and variable basis selection was mentioned in [6]. Independently, the same concept was also suggested as fashionable wavelet packets by other researchers.

For a given input signal, the tree structuring algorithm (TSA) recommends the best irregular subband tree structure consisting of two- or three-band prototype filter banks. The TSA considers both two- and three-band PR-QMF's in order to overcome the overlappings at the filters' transition frequencies, such as $\frac{\pi}{3}$, $\frac{\pi}{2}$, or $\frac{2\pi}{3}$. In particular, after justification, the input signal or any subband in the tree is decomposed into its orthogonal projections employing two- or three-band orthogonal subspaces. Therefore, the best irregular subband tree for the given input spectrum is generated in order to localize narrowband interference.

The TSA algorithm analyzes the energy distribution at each node of the subband tree, with the assumption of ideal filters used, and then, it decides whether to continue decomposition with additional branches or terminate the tree. A subband node is further decomposed if and only if the energy compaction value at this node exceeds a predefined threshold. The energy compaction measure quantifies the unevenness of the given signal spectrum. It is defined for an M-band linear transform as

$$G = \frac{\sigma_x^2}{\left[\prod_{i=1}^{M} \sigma_i^2\right]^{1/M}} \tag{3}$$

where σ_x^2 is the input variance, and $\{\sigma_i^2\}$ are the subband variances. The adaptive tree structuring algorithm (using the energy compaction measure) can be outlined as follows [6]:

1) Measure the power spectral density $P_{xx}(\omega)$ of the received signal.
2) a) Calculate subband variances σ_{2l}^2 and σ_{2h}^2 for the two-band split. Assume ideal filter banks employed, and find $G(2)$ (the energy compaction measure for the two-band split).

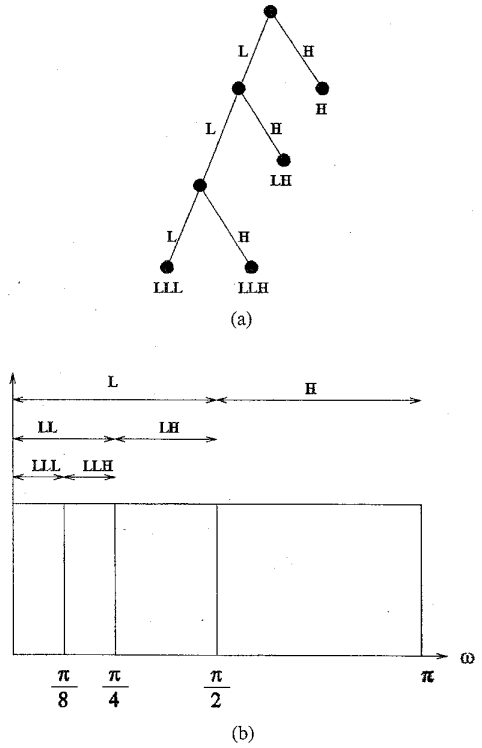

Fig. 4. (a) Three-level dyadic tree structure; (b) unequal bandwidth four-band spectra.

b) Calculate subband variances σ_{3l}^2, σ_{3b}^2, and σ_{3h}^2 for the three-band split. Assume ideal filter banks employed, and find $G(3)$ (the energy compaction measure for the three-band split).

3) If $G(2) \leq T$ and $G(3) \leq T$, then the spectral evenness exists. Stop tree structuring (where T is a predefined compaction threshold)

else proceed with the 2-band split
if $G(2) \geq G(3)$
or proceed with the 3-band split
which is the case if $G(2) < G(3)$.

4) Check the subband variances, and proceed splitting the interfered subband using two- or three-band splits. Do not split the uncontaminated subbands.
5) Repeat procedures 2, 3, and 4 until an evenness or flatness level is reached in the subspectra.

The operation of the adaptive subband tree structuring algorithm can be illustrated for the given spectral decomposition in Fig. 6(a). The TSA utilizes two-band lowpass/highpass prototype PR-QMF banks $[A_l(z), A_h(z)]$ and/or three-band lowpass/bandpass/highpass PR-QMF banks $[B_l(z), B_b(z), B_h(z)]$ in each generated stage. The adaptive TSA generates the corresponding irregular subband tree in Fig. 6(b), and the following analysis filters are obtained for the ideal spectral decomposition in Fig. 6(a):

$$H_1(z) = B_l(z)$$
$$H_2(z) = B_b(z)$$
$$H_3(z) = B_h(z)$$
$$H_4(z) = B_b(z)A_l(z^3) = H_2(z)A_l(z^3)$$

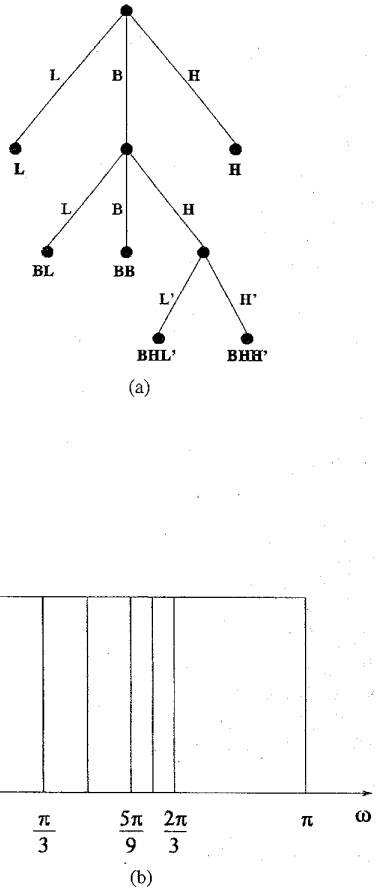

Fig. 5. (a) Irregular subband tree structure; (b) unequal bandwidth six-band spectra.

$$H_5(z) = B_b(z)A_h(z^3) = H_2(z)A_h(z^3)$$
$$H_6(z) = B_b(z)A_l(z^3)B_l(z^6) = H_4(z)B_l(z^6)$$
$$H_7(z) = B_b(z)A_l(z^3)B_b(z^6) = H_4(z)B_b(z^6)$$
$$H_8(z) = B_b(z)A_l(z^3)B_h(z^6) = H_4(z)B_h(z^6). \quad (4)$$

The corresponding synthesis filter functions $\{g_i(n)\}$ $[i = 1, \ldots 8]$ can be obtained as the time reversal of analysis filters $\{h_i(n)\}$ [8]. Clearly, while switching between two- or three-band filter banks, paraunitary conditions are always preserved. The adaptive subband tree structure avoids unnecessary decompositions by pruning. In particular, input signal-dependent, unequal bandwidth, paraunitary basis functions are obtained. The advantages of tree structuring over fixed subband trees are highlighted as

a) superior frequency resolution,
b) reduced interband energy leakage
c) reduced complexity of transform operations.

III. Adaptive Time-Frequency Exciser Algorithm

Fig. 7 displays the flow diagram of the proposed adaptive time-frequency (ATF) exciser algorithm. Unlike fixed transform techniques, the ATF exciser is capable of tracking and suppressing the time-varying, nonstationary interferences. The novelty of the ATF exciser is twofold. First, it evaluates the time features of the received signal in order to decide on the domain of the excision. A time window slides through the received signal and captures the samples that exceed an amplitude threshold. Then, the total number of the

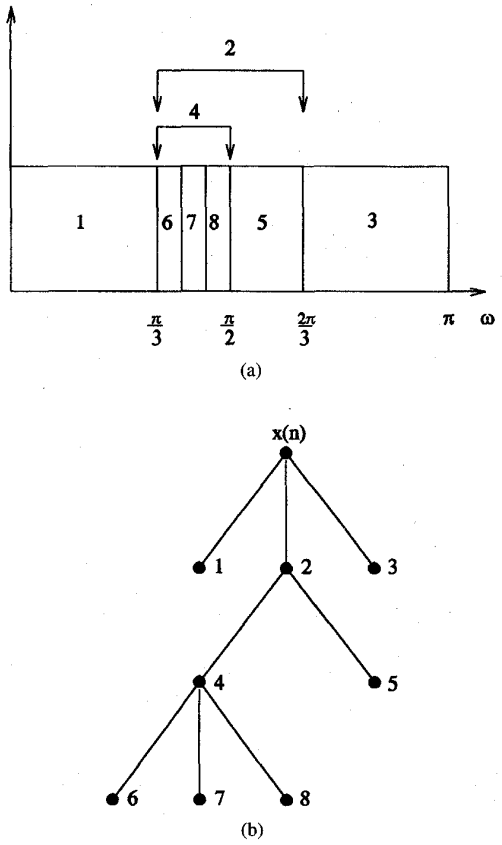

Fig. 6. (a) Unequal bandwith decomposition; (b) corresponding irregular subband tree.

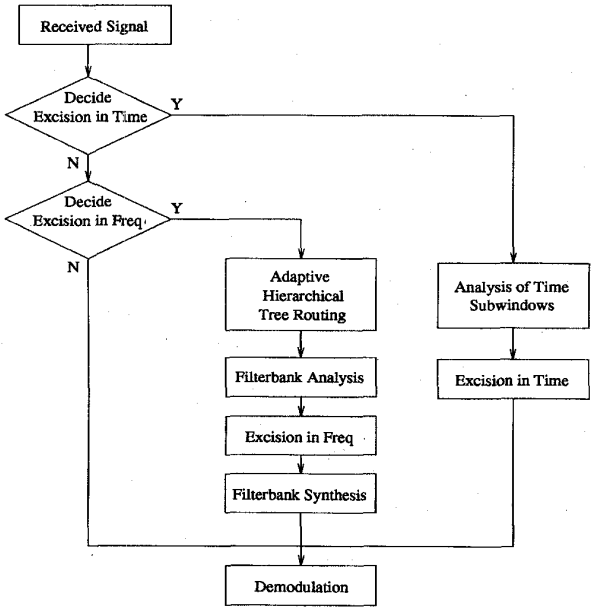

Fig. 7. Flow diagram of the proposed adaptive time-frequency exciser algorithm.

captured samples (N_c) is compared with a predetermined threshold (N_t). In fact, this threshold is a measure of energy distribution of the signal in the time domain. If N_c is less than or equal to N_t, then those

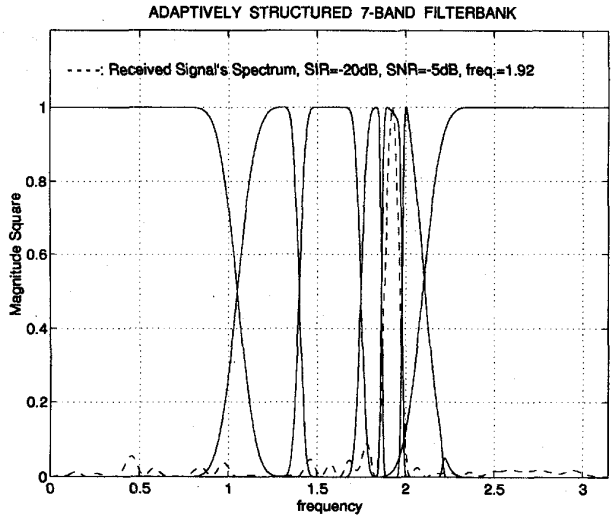

Fig. 8. Adaptive filter bank structure for single tone jammer case (tone frequency = 1.92 rad, SIR = −20 dB, SNR = −5 dB.

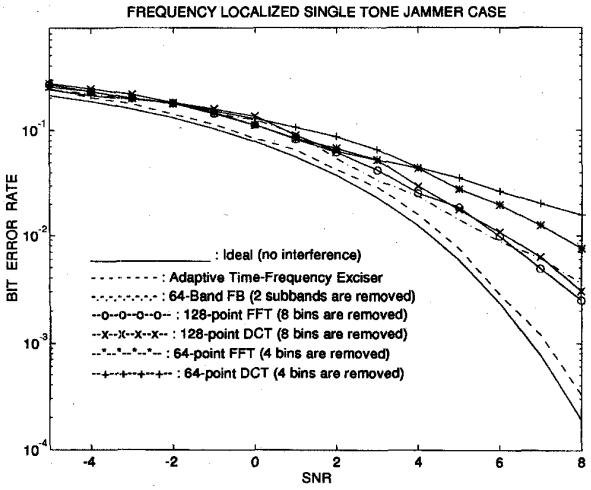

Fig. 9. Bit-error-rate curves for single tone jammer case (tone frequency = 1.92 rad, SIR = −20 dB.

interfered samples are nulled in the time domain. In particular, if the interference is time localized, such a simple time domain excision technique can outperform any transform domain technique. It is clear from the uncertainty principle that for a time localized interference, no transform domain excision technique can be justified.

The second novelty of the proposed ATF excision algorithm comes in when a frequency domain excision is decided after checking the frequency localization of the received signal. In this case, an adaptive subband transform is utilized for transform domain excision. As explained in the previous section, the TSA examines the spectrum of the received signal and defines the most proper subband tree structure. The contaminated or jammed subbands are discarded at the synthesis stage or directly filtered out by $H_i(z)G_i(z)$, which are localizing the interference. The subband tree structure changes whenever the input spectrum varies. The spectral decomposition is tracked to the variations of the input signal. Particularly, by its nature, an adaptive subband transform with justified splits prevents unnecessary amplitude distortions in the clean frequency bands.

It is meaningful to process the signal in the domain in which properties of the interference are more evident. If the interference

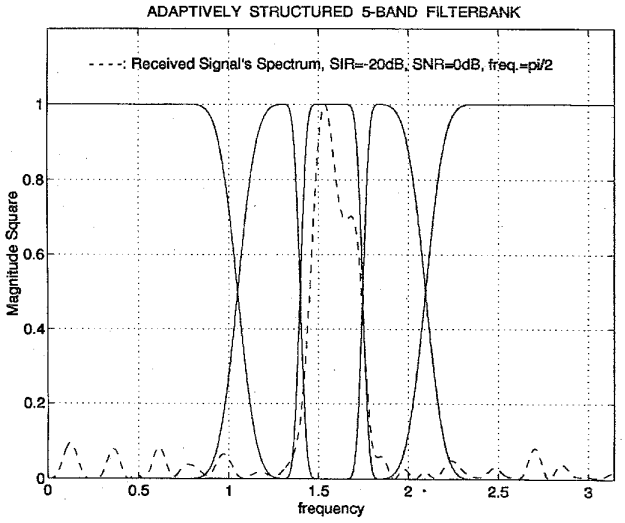

Fig. 10. Adaptive filter bank for structure for narrowband Gaussian jammer case (center freqency $= \frac{\pi}{2}$ rad, SIR $= -20$ dB, SNR $= 0$ dB).

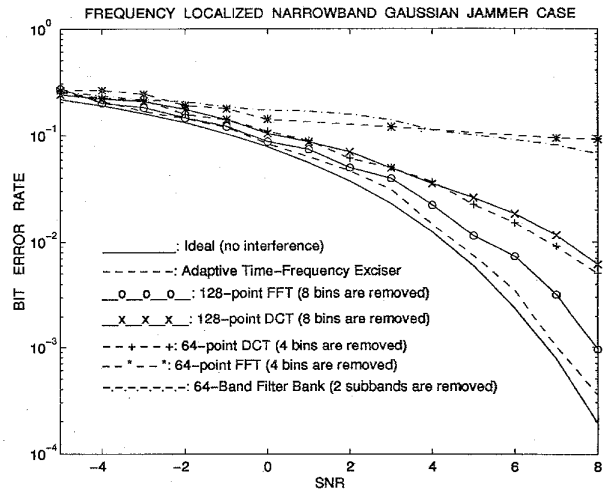

Fig. 11. Bit-error-rate curves for frequency localized narrowband Gaussian jammer case (center frequency $= \frac{\pi}{2}$ rad, SIR $= -20$ dB).

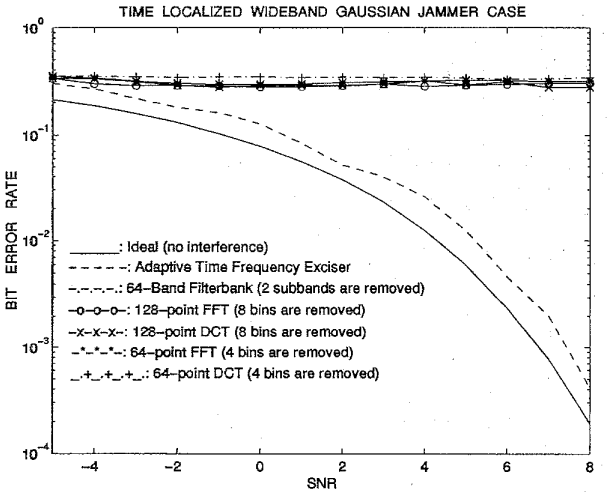

Fig. 12. Bit-error-rate curves for time localized wideband jammer case (10% duty cycle, SIR $= -20$ dB).

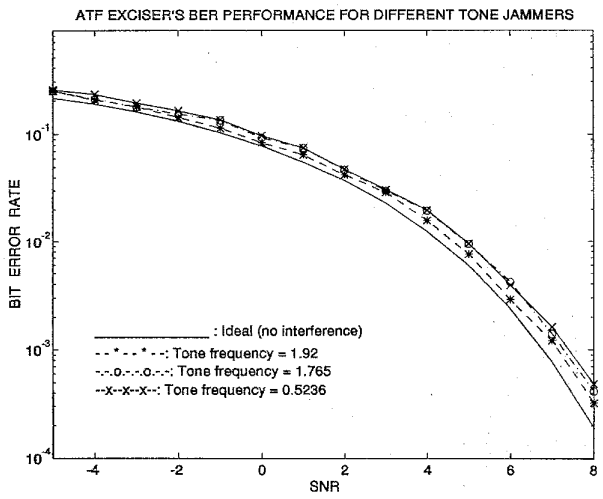

Fig. 13. Bit-error-rate curves of adaptive time-frequency tone jammers (SIR $= -20$ dB, $\omega_1 = 0.5236$ rad, $\omega_2 = 1.765$ rad, $\omega_3 = 1.92$ rad).

does not exist or localize in any domain, the received signal is passed directly to the PN demodulator, as in Fig. 7.

IV. Performance Comparisons and Conclusions

In order to evaluate the performance of a DSSS communications receiver employing the ATF exciser, a simulations package was created. The performance of the proposed ATF exciser along with DFT, DCT, and fixed 64-band PR-QMF bank based excisers is evaluated. A 63-chip maximum length PN code is used to spread the input bit stream. This provides a white spectrum for the transmitted signal. The baseband signal bandwidth is normalized to unity, and a BPSK modulation is assumed. The resulting DSSS signal is transmitted over an AWGN channel. Three types of interferences are considered: a single tone jammer, a narrowband Gaussian jammer, and a pulsed (time-localized) wideband Gaussian jammer.

A. Single Tone Jammer Case

A continuous sinusoidal interference with a frequency of 1.92 rad and uniformly distributed random phase ($\theta \in [0, 2\pi]$) is considered. The signal-to-interference power ratio is -20 dB. The ATF exciser employs a seven-band irregular filter bank structure given in Fig. 8. It has a fine spectral resolution around the interference frequency and minimum spectral leakage to uncontaminated bands. Fig. 9 displays the bit error rate (BER) performance of the ATF exciser-based DSSS system along with a few other fixed block transform exciser-based systems. The ideal curve represents the BPSK performance without any interference. The ATF exciser yields nearly optimal performance for sinusoidal interference. On the other hand, the fixed transforms (64-band filter bank, 64- and 128-point DFT and DCT) cannot guarantee good performance. Their performance depends on the frequency location of the interference signal. They perform relatively well if the frequency of the interfering tone exactly matches one of the transform bins.

B. Narrowband Gaussian Jammer Case

A continuous 10% bandwidth narrowband Gaussian interference with a center frequency of $\frac{\pi}{2}$ rad is considered. The signal-to-interference power ratio is -20 dB. The five-band, irregular filter

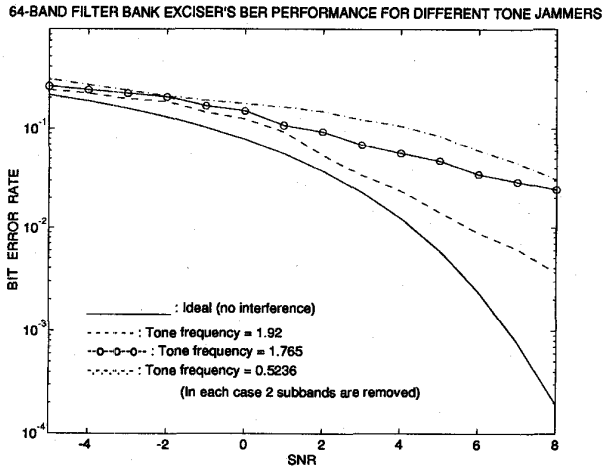

Fig. 14. Bit-error-rate curves of 64-band regular filter bank exciser for different frequency tone jammers (SIR $= -20$ dB, $\omega_1 = 0.5236$ rad, $\omega_2 = 1.765$ rad, $\omega_3 = 1.92$ rad).

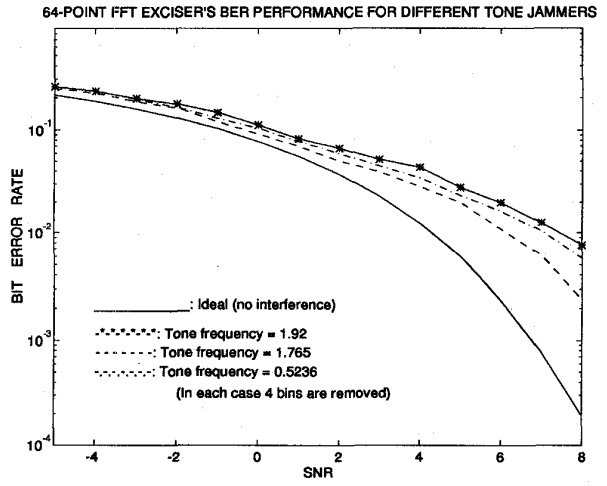

Fig. 15. Bit-error-rate curves of 64-point FFT exciser for different frequency tone jammers (SIR $= -20$ dB, $\omega_1 = 0.5236$ rad, $\omega_2 = 1.765$ rad, $\omega_3 = 1.92$ rad).

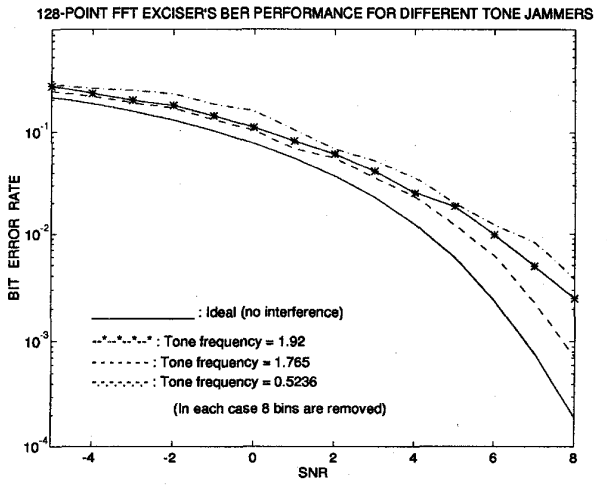

Fig. 16. Bit-error-rate curves of 128-point FFT exciser for different frequency tone jammers (SIR $= -20$ dB, $\omega_1 = 0.5236$ rad, $\omega_2 = 1.765$ rad, $\omega_3 = 1.92$ rad).

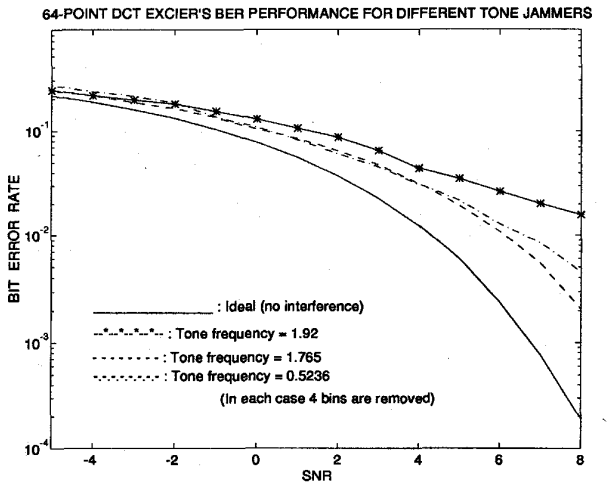

Fig. 17. Bit-error-rate curves of 64-point DCT exciser for different frequency tone jammers (SIR $= -20$ dB, $\omega_1 = 0.5236$ rad, $\omega_2 = 1.765$ rad, $\omega_3 = 1.92$ rad).

bank structure generated by the ATF exciser is displayed in Fig. 10. As seen in Fig. 10, the narrowband interference is confined in the third subband, and it is excised within this subband. The BER performances are shown in Fig. 11. The proposed ATF exciser yields the best performance compared with the other fixed transform-based excisers. The increase in the number of excised transform bins does not necessarily improve the BER performance since the desired components of the received spectrum are also removed during the excision.

It should be noted that frequency selectivity of fixed transforms might be improved at the expense of computational complexity. There have been several studies on these improvements in the literature [9], [10].

C. Nonstationary Wideband Gaussian Jammer Case

Fig. 12 displays the performance of ATF and fixed transform-based excisers for nonstationary, pulsed (time-localized) wideband Gaussian interference. This jammer is an on/off type that is randomly switched with a 10% duty cycle. The signal-to-interference power ratio is -20 dB. In this scenario, as expected, none of the fixed transform-based excisers is effective for interference suppression. However, the ATF exciser identifies the domain of the processing and successfully suppresses interference in the time domain. The dual treatment of signal properties in time and in frequency domains obviously brings significant performance improvements.

Robustness of Performance: One of the most important attributes of an interference suppression technique must be its robustness to time-varying signals. The BER performance results of the ATF exciser-based DSSS receiver for a single-tone jammer with varying frequency are displayed in Fig. 13. The similar results are displayed in Figs. 14–18 for the 64-band filter bank, 64-point, 128-point DFT, 64-point DCT, and 128-point DCT exciser-based DSSS receivers. It is seen from these plots that the ATF exciser-based system is very robust to the variations of the input signal, whereas the other conventional techniques are not.

An adaptive time-frequency exciser is proposed for DSSS communications. The proposed technique evaluates both the time and frequency domain properties of the received signal. The signal is

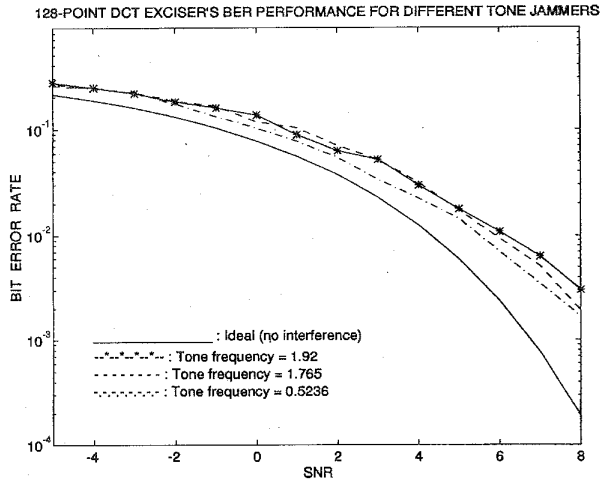

Fig. 18. Bit-error-rate curves of 128-point DCT exciser for different frequency tone jammers (SIR $= -20$ db, $\omega_1 = 0.5236$ rad, $\omega_2 = 1.765$ rad, $w_3 = 1.92$ rad).

processed in either the time or frequency domain, depending on the characteristics of the interference. For the time-domain excision, a sliding-nulling time window is effectively utilized. For frequency domain excision, adaptive subband transforms are used. They provide high spectral resolution (which is not possible for fixed transforms) in the region of interest. Hence, it reduces complexity by avoiding unnecessary decompositions. The domain switchability and adaptation properties make the ATF exciser a smart, robust, and meritful technique in spread spectrum communications.

REFERENCES

[1] R. E. Ziemer and R. L. Peterson, *Digital Communications and Spread Spectrum Systems*. New York: Macmillan, 1985.

[2] J. W. Ketchum and J. G. Proakis, "Adaptive algorithms for estimating and suppressing narrow-band interference in PN spread-spectrum systems," *IEEE Trans. Commun.*, vol. COM-30, pp. 913–924, May 1982.

[3] R. Iltis and L. Milstein, "Performance analysis of narrow-band interference rejection techniques in DS spread spectrum systems," *IEEE Trans. Commun.*, vol. COM-32, pp. 1169–1177, Nov. 1984.

[4] M. Medley, G. J. Saulnier and P. Das, "Applications of the wavelet transform in spread spectrum communications systems," in *Proc. Third NJIT Symp. Applicat. Subbands Wavelets*, Mar. 18, 1994.

[5] M. V. Tazebay and A. N. Akansu, "Progressive optimality in hierarchical filter banks," in *Proc. IEEE Int. Conf. Image Processing*, Nov. 1994, pp. 825–829.

[6] A. N. Akansu and Y. Liu, "On signal decomposition techniques," *Opt. Eng.*, vol. 30, no. 7, pp. 912–920, July 1991.

[7] M. V. Tazebay, A. N. Akansu, and M. J. Sherman, "A novel adaptive time-frequency excision technique for direct sequence spread spectrum communications," in *Proc. IEEE Int. Symp. Time-Frequency Time-Scale Anal.*, Oct. 1994, pp. 492–495.

[8] A. N. Akansu and R. A. Haddad, *Multiresolution Signal Decomposition: Transforms, Subbands, and Wavelets*. New York: Academic, 1992.

[9] W. W. Jones and K. R. Jones, "Narrowband interference suppression using filter bank analysis/synthesis techniques," in *Proc. MILCOM*, 1992, pp. 38.1.1–38.1.5.

[10] J. Gevargiz, M. Rosenmann, P. Das, and L. B. Milstein, "A comparison of weighted and nonweighted transform domain processing systems for narrowband interference excision," in *Proc. MILCOM*, 1984, pp. 32.2.1–32.3.4.

Direction-of-Arrival Estimation of Correlated Sources by Adaptive Beamforming

George V. Serebryakov

Abstract—**This correspondence has analyzed the capability of minimum energy optimum/adaptive beamformer to estimate the bearings of two closely spaced narrowband equal-energy correlated sources. The analytical expression for minimum angular separation for resolution of such sources as a function of the correlation coefficient, signal power, and the parameters of the adaptive processor is derived. The approach of spatial smoothing is considered. The simple problem of definition of optimal size of the subarray for highly correlated sources is examined. Results of computer simulations are included to support our analysis.**

I. INTRODUCTION

Use of the optimum/adaptive beamforming[1] in bearing estimation of closely spaced sources has become very popular due to its superresolution properties [1]-[4]. It has been shown that this method is capable of resolving two independent sources that are separated by an angle that is of the order of one standard beamwidth (sbw) and sometimes less. However, when some sources are fully or highly correlated (coherent), i.e., when one source is a scaled and delayed replica of another source, this method encounters significant difficulties concerned with signal cancellation effect [2], [3], [6], [7]. Note that coherent sources appear frequently in practical problems. A well-known example is the phenomenon of multipath propagation.

Several approaches have been developed for overcoming the problem of highly correlated arrivals. In their extensive study of direction-of-arrival estimation techniques, Evans, Johnson, and Sun [5] were the first to present a satisfactory solution to the problem of narrowband coherent sources. They showed that a subarray averaging technique known as "spatial smoothing" can be applied to combat coherence effects for direction finding. This idea was rediscovered by Shan *et al.* [8], [9].

The purpose of this paper is to obtain analytical estimates of the potential capability for adaptive beamforming in the presence of correlation among the sources as a function of coherence coefficient, signal power, and the parameters of the optimum processor. Next, we make a quantitative analysis of the effect of spatial smoothing on the source covariance matrix; we show that there is an optimal size of subaperture. Our resolution analysis is based on the assumption that the covariance matrix of the received signal will be determined exactly by averaging over an infinite period of time, thus enabling us to obtain an estimate of the limiting ability of resolution.

II. SIGNAL MODEL

Assume that L narrowband correlated (partially or fully) sources impinge on a linear array consisting of N equispaced omnidirectional sensors, and the directions of arrival (DOA's) of these sources are $\{\phi_1, \phi_2, \cdots, \phi_l\}$ with respect to the array normal. The output of the

Manuscript received July 24, 1993; revised April 21, 1995. This work was supported by SASPARC project of INTAS. The associate editor coordinating the review of this paper and approving it for publication was Dr. H. Fan.

G. Serebryakov is with the Research Institute of Applied Mathematics and Cybernetics, State University, Nizhny Novgorod, Russia.

IEEE Log Number 9415080.

[1] This beamforming algorithm, due to Capon [1], is often referred to as the maximum likelihood method (MLM) in the literature; however, actually the beam does not maximize a likelihood function.